

1 **Plant roots stimulate the decomposition of complex, but not simple,**
2 **soil carbon**

3
4
5
6
7
8 Jessica A. M. Moore*^a, Benjamin N. Sulman^b, Melanie A. Mayes^b, Courtney M.
9 Patterson^a, and Aimée T. Classen^c

10
11 ^a Department of Ecology & Evolutionary Biology, University of Tennessee, Knoxville, USA

12 ^b Environmental Sciences Division and Climate Change Science Institute, Oak Ridge National
13 Laboratory, Oak Ridge, TN, 37830, USA

14 ^c The Rubenstein School of Environment & Natural Resources, University of Vermont,
15 Burlington, VT, 05405, USA

16
17 *Corresponding author: Jbryan44@utk.edu
18

19 *Notice: This manuscript has been authored by UT-Battelle, LLC under Contract No. DE-AC05-*
20 *00OR22725 with the US Department of Energy. The United States Government retains and the*
21 *publisher, by accepting the article for publication, acknowledges that the United States*
22 *Government retains a non-exclusive, paid-up, irrevocable, world-wide license to publish or*
23 *reproduce the published form of this manuscript, or allow others to do so, for United States*
24 *Government purposes. The Department of Energy will provide public access to these results of*
25 *federally sponsored research in accordance with the DOE Public Access Plan*
26 *(<http://energy.gov/downloads/doe-public-access-plan>).*
27

This is the author manuscript accepted for publication and has undergone full peer review but has not been through the copyediting, typesetting, pagination and proofreading process, which may lead to differences between this version and the [Version of Record](#). Please cite this article as [doi: 10.1111/1365-2435.13510](https://doi.org/10.1111/1365-2435.13510)

This article is protected by copyright. All rights reserved

Author Manuscript

1 Section: Ecosystems Ecology

2 Editor: Dr Emma Sayer

3

4 **Abstract**

- 5 1. Roots release carbon into soil and can alleviate energy limitation of microbial organic
6 matter decomposition. We know little about the effects of roots on microbial
7
 - 8 ■ decomposition of different organic matter substrates, despite the importance for soil
9 carbon stocks and turnover. Through implementing root-microbe interactions, the
10 Carbon, Organisms, Rhizosphere, and Protection in the Soil Environment (CORPSE)
11 model was previously shown to represent dynamics of total soil carbon in temperate
12 forest field experiments. However, the model permits alternative hypotheses
13 concerning microbial-substrate affinity.
- 14 2. We investigated how root inputs affect decomposition of soil organic carbon (SOC)
15 with variable decomposability. We simulated SOC stocks in CORPSE and compared
16 microbial degradation of two substrates types with varying root-microbe interactions
17 under two alternative hypotheses that varied in microbial-substrate affinity. We
18 compared our modeled hypotheses to a forest field experiment where we quantified
19 decomposition of isotopically-labeled starch and leaf tissues in soils with manipulated
20 root access to microbes. We tested the hypothesis that decomposition of leaves would
21 be more sensitive to root inputs than decomposition of starch, corresponding to the
22 alternative model hypothesis.
- 23 3. In the field study, leaf decomposition increased with root density while starch
24 decomposition was unchanged by root density. Microbial biomass and enzyme
25 activity consistently increased with root inputs in CORPSE and the field study. Our
26 field experiment supported the CORPSE simulations with high microbial-substrate
27 affinity.
- 28 4. Roots stimulated microbial growth and enzyme production, which increased
29 degradation of more complex substrates such as leaf tissues. Substrates that were
30 easily decomposed, such as starch, may already be degrading at a maximum rate in
31 the absence of rhizosphere influence because their decomposition rate was unchanged
by root inputs. We found that the degree to which roots stimulate microbial

32 decomposition depends on the substrate being decomposed, and that root-microbe
33 interactions influenced SOC stocks in both our model and field experiment.
34 Environmental changes that alter root-microbe interactions could, therefore, alter soil
35 C stocks and biogeochemical cycling, and models of these interactions should
36 incorporate differential influence of rhizosphere inputs on different substrates.
37 **Keywords:** broadleaf boreal forest; ecosystem model; extracellular enzymes; plant-microbe
38 interaction; soil carbon; soil organic matter; stable isotopes

39 **Introduction**

40 Plants fix carbon (C) from the atmosphere to build biomass and much of that biomass enters soil
41 as leaf and root products. Although ample research has focused on aboveground inputs (Xu, Liu,
42 & Sayer, 2013), roots contribute 2.5-fold more C to soil than shoots (Rasse, Rumpel, & Dignac.,
43 2005). Given that soil is the largest stock of terrestrial C except for fossil reserves (Post,
44 Emanuel, Zinke, & Stangenberger, 1982; Jobbagy & Jackson, 2000), exploring how root inputs
45 affect soil C accumulation and feedbacks to the atmosphere is critical to understanding and
46 modeling the global C cycle (Phillips et al., 2012). Root inputs to soil in broadleaf boreal forests
47 are particularly important because roots comprise 39% of plant biomass, a greater portion than in
48 needle-leaf boreal, temperate, or tropical forests (Vogt et al., 1995). While researchers recognize
49 that roots are underrepresented in C models (Lynch, Matamala, Iversen, Norby, & Gonzalez-
50 Meler, 2013; McCormack et al., 2015), we are only beginning to understand and model how root
51 inputs alter soil C stocks (Keiluweit et al., 2015).

52 Root inputs from sloughed-off root cells, mucilage, exuded organic compounds, and dead
53 root tissues affect rates of soil C decomposition and accumulation. Microbial enzyme activity
54 increases with root exudation (Phillips, Finzi, & Bernhardt, 2011; Meier, Finzi, & Phillips,
55 2017). Root exudates prime microbial activity, where microbes release more C in CO₂ than is
56 contained in the exudates (Kuzyakov, 2010), in at least two ways: by increasing available
57 dissolved organic C and co-metabolism, and by lowering soil pH such that mineral-associated
58 organic matter is liberated from mineral surfaces (Blagodatskaya & Kuzyakov, 2008; Kuzyakov
59 et al., 2010; Keiluweit et al., 2015). As root exudates increase DOC, microbes are alleviated
60 from energy limitation and increase decomposition activity (Kuzyakov et al., 2010). Thus, both
61 exudate-driven mechanisms for decomposition translate to increased mineralization of soil C. In
62 fact, Crow et al. (2009) found that 11.5% – 21.5% of soil respiration in a temperate hardwood
63 forest was attributed to stimulation of microbial activity due to root inputs. While experiments
64 indicate that roots influence microbial activity (Lindahl, de Boer, & Finlay, 2010; Clemmensen
65 et al., 2013; Drake et al., 2013), incorporation of roots into soil C decomposition theory and
66 models has lagged.

67 Historically, models of soil organic matter decomposition have largely been based on C
68 pools with fixed turnover rates that do not accommodate the microbial decomposition feedbacks
69 necessary to simulate root input-microbial interaction influences on decomposition. While

70 microbial interactions have been incorporated into emerging soil C models, alternative structural
71 assumptions in these models lead to diverging responses to C inputs (Sulman et al., 2019).
72 Models of rhizosphere input effects are particularly sensitive to assumptions related to substrate
73 concentrations, microbial growth, and organic matter decomposition. Decomposition in these
74 models has been described using Michaelis-Menten enzyme kinetic theory where decomposition
75 rates increase with enzyme concentrations (e. g. Wang et al., 2015) or substrate concentrations
76 (e.g. Wieder et al., 2014) or in a more general framework using equilibrium chemistry
77 approximation (ECA) kinetics that incorporate both enzyme and substrate concentrations (Tang
78 and Riley, 2015; Tang 2015). An alternative approach incorporated in the CORPSE model
79 (Carbon, Organisms, Rhizosphere, and Protection in the Soil Environment; Sulman, Phillips,
80 Oishi, Shevliakova, & Pacala, 2014) assumes that microbial decomposition of soil organic matter
81 is determined by the amount of microbial biomass per unit substrate, rather than volumetric
82 concentration of substrate or enzymes. This approach allows the model to represent multiple
83 substrate types with different decomposition-related properties and is therefore useful for
84 simulating rhizosphere input effects.

85 An issue common to all of these model formulations is whether the effect of rhizosphere
86 inputs on microbial decomposition is substrate-specific (Fig. 1). In one formulation (Hypothesis
87 1), the decomposition rate of all compounds is controlled by the total concentration of microbial
88 biomass, meaning that all compounds have identical decomposition responses to microbial
89 growth. Alternatively (Hypothesis 2), rhizosphere input effects of different compounds may
90 saturate at different levels of microbial biomass, with simple compounds achieving their
91 maximum decomposition rate at low microbial biomass concentrations and decomposition of
92 more complex compounds increasing more slowly with respect to microbial biomass. These
93 alternative outcomes have important implications for the preservation or decomposition of labile
94 substrates in resource-limited environments such as deep soils or in highly-decomposed material
95 with low labile substrate concentrations. We used the CORPSE model in the context of a field
96 decomposition experiment to test which of these alternative hypotheses is a more appropriate
97 representation of microbial decomposition processes. We hypothesized that (1) the
98 decomposition rate of each substrate type is determined by the ratio of microbial biomass to total
99 unprotected soil C. In this case, changes in microbial biomass affect decomposition rate of all
100 substrates identically. Thus, simple and complex substrates would decompose slowly when

101 microbial biomass is small relative to total unprotected C, and decomposition rates of all
102 substrates would accelerate at the same proportional rate as microbial biomass increases. This
103 scenario represents a situation in which microbial decomposers assimilate a well-mixed
104 combination of substrates. Alternatively, we hypothesized that (2) the decomposition rate of each
105 substrate is related to microbial biomass to different degrees for different substrates. That is,
106 simple C could be decomposed rapidly given low microbial biomass while complex C could be
107 less sensitive to changes in microbial biomass. This hypothesis represents a scenario in which
108 substrates are distributed unevenly and can be accessed separately by decomposers. Microbes
109 can target substrates that are present in small amounts but have properties that are highly
110 favorable for assimilation. The overall implication of our model hypothesis (i) is that the effect
111 of rhizosphere input on microbial decomposition are universal for all substrates, and the
112 implication of model hypothesis (ii) is the effect of rhizosphere inputs can vary for different
113 substrates.

114 We empirically investigated how soil C decomposition responded to root inputs in a
115 broadleaf boreal forest. Root exudation is known to vary with root density (Phillips et al., 2011),
116 thus we used root density as a proxy for both exudation and root litter inputs. We simulated soil
117 C processes using the CORPSE model to determine differential responses of simulated SOC
118 across a gradient of root inputs. CORPSE divides SOC into different types, including one that is
119 easily decomposed and assimilated (i.e., simple) by microbes and a second that is less easy to
120 decompose (i.e., complex). We compared the CORPSE-simulated C pool responses to
121 measurements in a field study where we experimentally generated a gradient of root density and
122 tracked decomposition of leaf material and starch. Using this combined model-experiment
123 approach, we answered the question: how does microbial activity and decomposition of soil C
124 that is chemically simple or complex respond to a gradient of root density? We hypothesized
125 that: (i) C mineralization rates of leaf material would be lower than those of starch, (ii) microbial
126 biomass would increase with root density, (iii) microbial enzymatic activity would increase with
127 root density, and (iv) C mineralization rates from leaf material would increase with higher root
128 density but C mineralization rates from starch would be constant with root density. After six
129 weeks of field incubation, we measured $^{13}\text{CO}_2$ respired from soils amended with ^{13}C -labeled leaf
130 material or starch, microbial biomass, and enzymatic decomposition activity. Our model

131 simulations and experiment suggested that root density influenced decomposition of chemically
132 complex C more than simple C.

133 **Methods**

134 CORPSE simulations

135 The CORPSE model simulates soil C cycling using an explicitly defined microbial
136 biomass pool that drives the decomposition rate of multiple organic substrates (Fig. 2). See
137 Supplemental Table S2 for model parameter values used in our simulations. Organic matter is
138 divided into three chemically-defined forms, which can be either protected or unprotected.
139 Protected organic matter is inaccessible to microbial decomposition through chemical sorption to
140 mineral surfaces or occlusion within micro-aggregates. Unprotected organic matter can be added
141 as litter or root exudate inputs, decomposed by microbial action, or protected:

$$143 \frac{dC_{U,i}}{dt} = I_{C,i} - D_i + T_M - \frac{dC_{P,i}}{dt} \quad (\text{eqn. 1})$$

144
145 where $C_{U,i}$ is unprotected C; $I_{C,i}$ is external inputs of C (including litter deposition and root
146 exudation); D_i is decomposition rate; T_M is microbial necromass production; and $\frac{dC_{P,i}}{dt}$ is net
147 transfer of C to or from the protected state. i refers to chemically-defined types, which can be
148 chemically simple plant-derived material (representing compounds like glucose or amino acids
149 that are readily decomposed), chemically resistant (representing compounds like lignin or
150 complex microbially-produced chemicals), or readily decomposable microbial necromass.
151 Protected C is formed from unprotected organic matter and converted back to unprotected form
152 at first-order rates:

$$154 \frac{dC_{P,i}}{dt} = C_{U,i} \cdot k_{P,i} - \frac{C_{P,i}}{\tau_P} \quad (\text{eqn. 2})$$

155
156 Note that this model formulation does not currently include rhizosphere effects on the turnover
157 of protected C. The decomposition flux is controlled by microbial biomass (B_M), temperature
158 (T), and volumetric soil water content (θ). The effect of microbial biomass on decomposition
159 was defined in two alternate ways, reflecting Hypothesis 1 (equation 3a), and Hypothesis 2
160 (equation 3b).

161

162
$$D_i = V_{max,i}(T) \cdot \left(\frac{\theta}{\theta_{sat}}\right)^3 \left(1 - \frac{\theta}{\theta_{sat}}\right)^{2.5} \cdot C_i \frac{B_M / \sum_i C_{U,i}}{B_M / \sum_i C_{U,i} + k_C}$$
 (eqn. 3a)

163

164

165
$$D_i = V_{max,i}(T) \cdot \left(\frac{\theta}{\theta_{sat}}\right)^3 \left(1 - \frac{\theta}{\theta_{sat}}\right)^{2.5} \cdot C_i \frac{B_M / C_{U,i}}{B_M / C_{U,i} + k_C}$$
 (eqn. 3b)

166

167 where θ_{sat} is the saturation level of θ and $V_{max,i}$ is the substrate-specific maximum decomposition
168 rate. Increases in B_M driven by growth on substrates with high carbon use efficiency and V_{max}
169 drive priming effects in the model (see below). Note the key difference between equations 3a and
170 3b: In equation 3a, decomposition rate is determined by the ratio of B_M to C_U summed over all
171 substrate types, while in equation 3b decomposition rate is determined for each substrate type
172 $C_{U,i}$ by the ratio of B_M to the amount of that substrate type.

173

174

175

176
$$V_{max,i}(T) = V_{max,ref,i} \times \exp\left(-\frac{E_{a,i}}{R} \left(\frac{1}{T} - \frac{1}{T_{ref}}\right)\right)$$
 (eqn. 4)

177

178 where $V_{max,ref,i}$ is a maximum decomposition rate specific to each chemically-defined organic
179 matter type, $E_{a,i}$ is activation energy for each organic matter type, and R is the ideal gas constant
180 ($8.31 \text{ J K}^{-1} \text{ mol}^{-1}$).

181

182

183

184
$$\frac{dB_M}{dt} = \sum_i (D_i CUE_i) - \frac{B_M - B_{min}}{\tau_{mic}}$$
 (eqn. 5)

185

186 where CUE_i is C use efficiency for substrate i and τ_{mic} is the microbial biomass turnover time.
187 The complex C is defined in CORPSE as having low maximum decomposition rate (V_{max}) and
188 low microbial C use efficiency (CUE) which is comparable to leaf material, whereas simple C
189 has high V_{max} and high CUE which is comparable to starch. We defined starch as a simple

190 substrate because it is a pure carbohydrate chain, and leaf material as complex because it
191 contains many compounds bound in a lignocellulose matrix. Because simple C has a higher
192 associated CUE and V_{\max} than complex C, it promotes microbial growth, thereby accelerating
193 decomposition and driving priming effects for all substrates. B_{\min} is minimum microbial
194 biomass, defined as a fraction of total unprotected C:

$$195$$
$$196 \quad B_{\min} = f_{B,\min} \sum_i C_{U,i} \quad (\text{eqn. 6})$$
$$197$$

198 Microbial biomass turnover is divided into maintenance respiration (R_{maint}), which is converted
199 directly to CO_2 , and necromass production (T_M). The division between R_{maint} and T_M is
200 controlled by a parameter ϵ_t :

$$201$$
$$202 \quad R_{\text{maint}} = \frac{B_M - B_{\min}}{\tau_{\text{mic}}} (1 - \epsilon_t) \quad (\text{eqn. 7})$$
$$203$$

$$204 \quad T_M = \frac{B_M - B_{\min}}{\tau_{\text{mic}}} (\epsilon_t) \quad (\text{eqn. 8})$$
$$205$$

206 Total CO_2 production rate is the sum of maintenance respiration and respiration derived from
207 decomposition processes:

$$208$$
$$209 \quad \frac{d\text{CO}_2}{dt} = R_{\text{maint}} + \sum_i ((1 - \text{CUE}_i) D_i) \quad (\text{eqn. 9})$$
$$210$$

211 Rhizosphere input simulations

212 We parameterized the model using soil texture measured at our experimental field site
213 (described below, in Field Study) and measured soil temperature and moisture from a nearby
214 monitoring station (Hanson et al., 2011). Total C inputs to the soil were estimated to be 1.5 mg C
215 $\text{g soil}^{-1} \text{y}^{-1}$, composed of 30% simple C and 70% complex C, and the model was spun-up with
216 repeating inputs and meteorological drivers until soil C pools reached a steady state. We then
217 simulated decomposition across a gradient of root density that was representative of the
218 measured variability of root density at our site. Root exudation was calculated based on root
219 length using an estimated growing-season value of $0.25 \mu\text{g C (cm root length)}^{-1} \text{hour}^{-1}$ (Phillips

220 et al., 2011; Yin et al., 2013). Root exudation was assumed to have a sinusoid pattern through the
221 year, with maximum exudation rate occurring in August of each year (Phillips et al., 2011). Root
222 exudates were assumed to be entirely composed of simple C. This assumption is a simplified
223 representation of exudate composition, which may also include organic acids that can liberate
224 mineral-bound soil C thus further alleviating microbial C limitation (Keiluweit et al., 2015). Our
225 simplified representation of exudates therefore yields more conservative results because it limits
226 the source of microbial priming to simple C compounds (e.g., glucose).

227 Field Study

228 The field study was conducted at Marcell Experimental Forest (47°30'26.73", -93°27'15.68")
229 located 40 km north of Grand Rapids, Minnesota, USA. The average annual temperature was
230 3°C and average precipitation was 785 mm yr⁻¹. Our study site was located in a 40 m × 40 m area
231 within a forest primarily composed of bigtooth aspen (*Populus grandidentata*), trembling aspen,
232 (*Populus tremuloides*) and paper birch (*Betula papyrifera*). The dominant understory plants were
233 bracken fern (*Pteridium aquilinum*), dwarf raspberry (*Rubus pubescens*), round-leaved dogwood
234 (*Cornus rugosa*), and beaked hazel (*Corylus cornuta*). Soils were pH 5.0 ± 0.44 with a bulk
235 density of 1.26 ± 0.41 g cm⁻³ and are fine, sandy loams classified as Warba series (Kolka, Grigal,
236 Nater, & Verry, 2001).

237 We manipulated root access to soil microbes by constructing mesocosms made from a 15
238 cm long, 5 cm diameter PVC pipe. Two 10.5 cm × 8 cm openings were cut along the length of
239 the pipe, one on each side. We covered these openings, as well as the bottom of the pipe, with
240 stainless steel mesh attached with rivets and nutrient-free glue (Household Goop, Eclectic
241 Products, Eugene, USA). We covered 135 mesocosms with one of three mesh sizes: 1.45 mm (n
242 = 45), 38 μm (n = 45), or 5 μm (n = 45). We intended to exclude roots from fine-mesh
243 mesocosms and allow root access to soil with large-mesh mesocosms (Johnson, Leake, & Read,
244 2001; Langley, Chapman, & Hungate, 2006; Phillips et al., 2012; Rewcastle et al. In press).
245 However, a previous study showed the mesh design does not generate absolute root exclusion in
246 all forest types (Moore et al., 2015). Mesocosms in the previous study varied in root density, thus
247 we analyzed our data across a gradient of root density.

248 On May 12, 2014, we installed mesocosms randomly throughout the study site. We
249 removed any organic horizon material and excavated the top 15 cm of mineral soil using a 5 × 15
250 cm hammer corer (AMS, Inc., American Falls, USA). The top 15 cm included only the A

251 horizon. We removed visible roots to avoid a litter fertilization effect, and then filled each
252 mesocosm with this root-free native soil. We placed each mesocosm in the hole from which it
253 was collected and ensured the mesh was completely below the soil surface. Mesocosms were
254 placed at least 0.5 m away from each other.

255 In-situ ^{13}C -starch and ^{13}C -leaf material incubation

256 Adding stable isotopes to soil enabled us to track microbial activity within specific C
257 pools. We applied a 99 atom-% ^{13}C labeled algal starch (Cambridge Isotope Laboratories,
258 Tewksbury, MA, USA) and a >97 atom-% ^{13}C labeled ground tulip-poplar (*Liriodendron*
259 *tulipiferae*) leaf material (IsoLife, Wageningen, Netherlands). We suspended 5 mg of powdered
260 starch (0.58 mg C) or ground leaf material (2.3 mg C) in 30 mL of deionized water and injected
261 into mesocosms that contained approximately 350 g soil. The amount of C added to soil from
262 starch ($1.6 \mu\text{g C g}^{-1}$) or leaf material ($6.6 \mu\text{g C g}^{-1}$) was large enough to have a traceable label but
263 small enough to not fertilize the soil, which contained on average 20 mg C g^{-1} soil at our site and
264 is a similar amount to other C tracer field studies (Zak & Kling, 2006). The injections were
265 conducted on June 24, 2014, six weeks after installing the mesocosms. We injected the starch
266 suspension into 45 mesocosms (15 of each mesh size) and the leaf solution into 45 mesocosms
267 (15 of each mesh size). To control for moisture addition and disturbance, we injected deionized
268 water into 21 starch-control mesocosms (7 of each mesh size) collected on the same day as
269 starch-addition mesocosms, and into 24 leaf-control mesocosms (8 of each mesh size) collected
270 on the same day as leaf-addition mesocosms. Mesocosms injected with the starch suspension
271 were sampled for $^{13}\text{CO}_2$ on days 1, 2, 3, 4 and 5 after injection, and those with the leaf
272 suspension were sampled on days 2, 4, 6, 10, and 20 after injection. We sampled gasses across
273 several days because we were unsure which day CO_2 flux would peak and this timeframe
274 ensured we would capture peak microbial respiration of the ^{13}C -labeled substrate (Zak & Kling,
275 2006). To collect gas samples for $^{13}\text{CO}_2$ analysis, we capped the cores with a tightly fitting 5 cm
276 diameter PVC cap fitted with a rubber septum. After 20 min, we used a syringe to draw a 15 mL
277 sample of gas from the cap and injected the sample into a 12 mL Exetainer vacuum vial (Labco
278 Limited, Lampeter, UK). One gas sample per sampling day was taken from the cores. At the
279 beginning and end of each sampling day two ambient samples were taken to establish
280 background levels of $^{13}\text{CO}_2$. All $^{13}\text{CO}_2$ samples were analyzed at the UC Davis Stable Isotope
281 Facility (Davis, USA) using a ThermoScientific PreCon-GasBench system interfaced to a

282 ThermoScientific Delta V Plus isotope ratio mass spectrometer (ThermoScientific, Bremen,
283 USA). We removed all starch and starch-control mesocosms on June 29, 2014 and all leaf and
284 leaf-control mesocosms on August 4, 2014. We placed the contents of mesocosms in a plastic
285 bag, transported them in a cooler on ice, and stored at 4°C until they were analyzed.

286 To quantify root density, we removed unsieved soil from the mesocosms and visually
287 inspected soils for roots. We used forceps to collect fine (<2 mm) roots and placed field-moist
288 root mass into a clear-bottomed reservoir filled with water to a depth of approximately 2 cm. We
289 scanned the roots in the reservoir on a photo scanner at 300 dpi resolution. We cropped the
290 images to remove the border created by the reservoir, and then calculated root length using the
291 Morphology plug-in and IJ Rhizo script for ImageJ software (Lobet & Draye, 2013). Root
292 density is equal to root length per volume soil.

293 We analyzed microbial biomass C (MBC) within 48 hours of soil collection using the
294 chloroform fumigation-extraction method (Vance, Brooks, & Jenkinson, 1987), allowing
295 fumigated samples to incubate at room temperature for 5 days. All samples were stored at 4°C
296 until analysis. We measured C of the samples on a total organic carbon analyzer (TOC-V CPH
297 Total Organic Carbon Analyzer, Shimadzu Scientific Instruments, Columbia, USA). Microbial
298 biomass C was calculated using a correction factor of 0.38 (Voroney, Brooks, & Beyaert, 2007).

299 We analyzed the potential enzyme activity of our soils using methods described by Bell
300 et al. (2013) within 48 h of collection. Briefly, we mixed 2.75 g of field moist soil (sieved to 2
301 mm) with 91 mL of 50 mM sodium acetate buffer at pH 5 using an immersion blender. We
302 pipetted 800 µL of soil slurry into a column on a deep (2 mL) 96-well plate that contained 0 -100
303 µM of methylumbelliferyl (MUB) to establish a standardized MUB reaction for each soil
304 sample. We then pipetted 800 µL of the soil slurry into a separate plate and added 200 µL of 4-
305 MUB-β-D-glucoside (β-gluc), 4-MUB-cellobioside (CBH), 4-MUB-N-acetyl-β-D-glucosaminide
306 (NAG), or 4-MUB-phosphate (PHOS) to each soil sample. β-gluc and CBH are hydrolytic
307 enzymes that work in concert to break down cellulose into glucose, and NAG and PHOS are
308 used by microbes to acquire nitrogen and phosphorus, respectively. We sealed each plate with a
309 plate mat, agitated vigorously by hand, then incubated the MUB standard and sample plates in
310 the dark at room temperature for 3 h. Using a fluorometer/spectrophotometer (Synergy HT,
311 Biotek Inc, Winooski, USA) we measured fluorescence at an excitation wavelength of 365 nm
312 and an emission wavelength of 450 nm.

313 Statistical Analyses

314 We tested for the effects of root density on microbial activity using linear regressions.
315 Data were log-transformed when necessary to meet assumptions of normality. We tested whether
316 roots affected microbial metabolism of different pools of C by regressing root density against
317 $\delta^{13}\text{C}$ captured in CO_2 and included C source (starch or leaf material) as a co-variate. We
318 determined the effect of roots on microbial biomass by regressing root density with MBC, and
319 the effect of roots on microbial activity by regressing root density with each of four enzyme
320 activities. All regressions were performed separately and were considered significant at $\alpha = 0.05$.
321 We report the probability that empirical responses were not related to root density (P), ratio of
322 variance among empirical response groups (F), and coefficients of correlation between empirical
323 responses and root density (r^2). All analyses were performed in R (R Core Team, 2016) using the
324 basic package and normality was tested for using the package fBasics (Rmetrics Core Team,
325 2014).

326 Results

327 CORPSE Simulations

328 Model simulations showed a strong effect of root density on microbial biomass and
329 decomposition rates, and projected significant differences in simple C decomposition between
330 the alternative hypotheses. Root exudation in the simulations with the highest root density
331 increased the decomposition rate of complex C by more than 120% under both hypotheses (Fig.
332 3a). In contrast, the decomposition rate per unit mass of simple C declined slightly (by less than
333 1%) as root density increased under Hypothesis 2 while increasing similarly to complex C under
334 Hypothesis 1. The decline in simple C turnover rate with higher root density under Hypothesis 2
335 occurred because the amount of total simple C increased with additional root inputs, whereas the
336 amount of total complex C was unchanged by root inputs. The accelerated decomposition rate of
337 complex C was driven by a large increase in simulated microbial biomass concentration at higher
338 root densities (Fig. 3b, S1). Simulated microbial biomass across the gradient of root density was
339 consistent with measurements (see below).

340 Field Study

341 Roots affected decomposition of leaf-C differently than starch-C. Root density in field
342 mesocosms ranged from 0.1 to 523.3 mm g^{-1} dry soil (mean = 63.4 mm g^{-1} , median = 14.8 mm g^{-1})
343 and it did not vary with mesocosm mesh size (P = 0.15, F = 1.93), soil C:N (P = 0.67, F =

344 0.18), or soil pH ($P = 0.60$, $F = 0.27$; Supplemental Table S1). The effect of root density on
345 $\delta^{13}\text{CO}_2$ was different for starch and leaf material ($P = 0.009$, $F = 7.24$). The $\delta^{13}\text{CO}_2$ captured
346 from decomposed labeled leaf material increased with root density, while decomposition of
347 labeled starch was not correlated with root density ($P = 0.009$, $R^2 = 0.51$, Fig. 3c). When we
348 standardized the $\delta^{13}\text{CO}_2$ respired given the different initial C concentrations of leaf material and
349 starch, we found that $\delta^{13}\text{CO}_2$ respired from the substrates was related to root density differently
350 ($P = 0.01$, $F = 6.72$). For both substrates, decomposition rates peaked two days after the
351 substrates were added to soils.

352 Root density increased MBC and C-degrading enzyme activity. Microbial biomass C
353 increased with root density ($P = 0.001$, $R^2 = 0.12$, Fig. 3d). As we anticipated, the effect of root
354 density on MBC did not vary with C source because of the trace amount of substrate C added to
355 each mesocosm ($P = 0.61$, $F = 0.49$). β -glucosidase potential activity per unit soil C increased
356 with root density ($P = 0.01$, $R^2 = 0.17$, Fig. 4a), but was not affected by C source ($P = 0.23$, $F =$
357 1.48). Cellobiohydrolase potential activity was not related to root density ($P = 0.10$, $R^2 = 0.04$,
358 Fig. 4b), and did not vary with C substrate ($P = 0.64$, $F = 0.45$). Root density was not correlated
359 with the nutrient-acquiring enzymes NAG ($P = 0.13$, $R^2 = 0.01$) or PHOS ($P = 0.08$, $R^2 = 0.02$).
360 PHOS rates were marginally higher in leaf-addition mesocosms and lower in starch-addition
361 mesocosms ($P = 0.03$, $F = 3.47$), but a post-hoc Tukey HSD test suggested that neither were
362 different from control ($P = 0.26$ for leaf material v. control, $P = 0.59$ for starch v. control).
363 PHOS rates were also similar to control with starch-addition (Tukey HSD: $P = 0.88$) and were
364 higher than control for leaf-addition (Tukey HSD: $P = 0.03$). Overall, we found that roots
365 stimulated microbial biomass and C-degrading activity but not nutrient-acquiring activity.

366

367 Discussion

368 Root inputs stimulate microbial decomposition (Phillips et al., 2011; Keiluweit et al., 2015), but
369 modeling approaches and previous empirical studies have not definitively established to what
370 extent root-microbe interactions differently influence the decomposition of different SOC
371 fractions. We addressed this uncertainty by comparing simulations from the rhizosphere model
372 CORPSE with an experiment conducted in a broadleaf boreal forest because boreal forests
373 harbor large pools of C that is potentially climate-sensitive (Clemmensen et al., 2013; Bradshaw
374 & Warkentin 2015; Crowther et al., 2016). We demonstrated that root inputs were correlated

375 with decomposition of complex SOC, while there was negligible correlation between root
376 density and decomposition of simple SOC. Thus, our experimental results supported Hypothesis
377 2, indicating that substrates decompose at different rates depending on root-microbe interactions.
378 Decomposition of complex SOC in CORPSE under both hypotheses increased as root inputs
379 increased microbial activity and biomass, a result that was supported by our field experiment.
380 We measured higher efflux of $^{13}\text{CO}_2$ originating from leaf material where root density was high
381 compared to low and found no relationship between $^{13}\text{CO}_2$ efflux from starch and root density.
382 Overall, both our empirical and model results demonstrated that complex C was more sensitive
383 to root-microbe interactions than simple C and suggested that model formulations consistent with
384 these differential effects on different substrates should be used in simulations of rhizosphere
385 impacts on soil C.

386 Previous studies find that rhizosphere interactions are important in the context of deep
387 soils (Hicks Pries et al., 2018), Arctic soils (Hartley et al., 2012), and ecosystem-scale C and
388 nutrient cycling (Finzi et al., 2015), and that rhizosphere interactions can drive global-scale
389 sensitivity of soil C stocks to changes in climate and ecosystem productivity (Sulman et al.,
390 2014; Sulman et al., 2019). Improving model representations of rhizosphere interactions is
391 important for enhancing the predictive capacity of ecosystem models. In particular, our results
392 suggest that in substrate-limited environments like deep soils, preservation of labile C substrates
393 may be limited since external resource subsidies are not required for their decomposition. Thus,
394 even in deep soils the preservation of organic material due to resource limitation may be limited
395 to more complex substrates.

396 Complex C decomposition increased with root inputs in the CORPSE simulations. To
397 directly compare with this modeled result, we would need to measure turnover of complex SOC
398 in isolation from other SOC pools, but measuring turnover of distinct pools of SOC is a
399 challenge in field studies. We did, however, measure mineralization of two types of C using
400 isotopically labeled substrates. We found increased $^{13}\text{CO}_2$ from leaf material with increasing root
401 density, which suggested increased microbial activity and turnover of complex C. Our result
402 corroborates a temperate forest tree girdling study. When root inputs to soil were cut off, leaf
403 litter decomposition was reduced by 40% compared to control plots (Brzostek, Dragoni, Brown,
404 & Phillips, 2015). CORPSE simulations suggested that root exudate inputs alleviated C
405 limitations to microbial biomass and thereby enhanced complex C decomposition by stimulating

406 the growth of microbial biomass. Root inputs were correlated with microbial biomass here and in
407 a temperate pine forest (Phillips et al., 2011), but neither of these studies isolated the responses
408 of different SOC fractions. We hypothesize that microbes specializing on leaf material
409 degradation increased decomposition activity in presence of leaf material, and these microbes
410 were sensitive to root inputs. While it is known that root-associated microbial communities are
411 distinct from those in bulk soil (DeAngelis et al., 2009; Shi et al., 2011; Lou et al., 2014),
412 whether these communities differentially decompose pools of C remains unknown.

413 In contrast to complex C, simple C decomposition did not respond to higher root density
414 in this boreal forest experiment. The CORPSE model simulations suggested that this response
415 was more consistent with the assumption that microbial access and assimilation of these simple
416 C compounds did not benefit from additional energy subsidies or other rhizosphere effects. In
417 other words, the rapid decomposition rate and high CUE supported enough microbial biomass to
418 decompose simple C at a maximal rate even at low concentrations of simple C. As a result, the
419 simulated relationship between microbial biomass and simple C decomposition reached a
420 saturation point at low levels of root inputs (Figure 1b; Supplemental Fig. S1). These results
421 suggest that in environments composed mostly of complex material such as needleleaf-
422 dominated litter layers, even small amounts of labile C could significantly stimulate microbial
423 decomposition of more complex substrates. Under Hypothesis 1, labile C decomposition was
424 slower when labile C concentration was low relative to complex C (in the absence of root
425 exudates). Our study suggested that this assumption was incorrect, and that instead labile C could
426 decompose rapidly, enhancing microbial growth, even at low concentrations (Hypothesis 2).

427 Nutrient limitation is a potential hypothesis that may resolve the different responses of
428 complex and simple C decomposition rates to root inputs in our study. Microbes may
429 preferentially utilize inputs that contain C and N, rather than C-rich inputs, to meet their
430 stoichiometric demands (Drake et al., 2013). We did not explore nutrient limitation of
431 decomposition in CORPSE, and we have not experimentally found a relationship between
432 microbial N or P acquisition and root density or decomposition of complex or simple C. Yet,
433 others have reported increased N-acquiring activity with root exudation (Phillips et al., 2011;
434 Meier et al., 2017) and higher rates of N immobilization in presence of roots (Holz et al., 2016).
435 In a temperate pine forest, proteolytic activity doubled with additions of root exudate-like
436 compounds to soil (Meier et al., 2017). We may not have captured any effect of root inputs on

437 nutrient-acquisition because we measured only two of the many nutrient-acquiring enzymes that
438 microbes produce. Alternatively, the in-growth mesocosm installation likely disturbed soil
439 aggregates, thus altering nutrient pools, and the disturbed microbial communities may have
440 altered community structure and functional capacity for decomposition (Franzluebbers, 1999).
441 We studied decomposition within in-growth mesocosms relative to disturbance-control
442 mesocosms. Rhizosphere interactions in undisturbed soils may differ from those we have
443 demonstrated within in-growth mesocosms due to the experimental manipulations we imposed.
444 For a more comprehensive microbial activity investigation, we recommend that future studies
445 take advantage of -omics technologies and gene expression assays targeting production of
446 nutrient transport proteins (Treseder & Lennon, 2015).

447 While our study focused on the decomposition of SOC compounds with different
448 chemical complexities, a large fraction of SOC is physically protected from microbial
449 decomposition via associations with mineral particles or small aggregates. Discerning root-
450 microbe interactive effects on decomposition of C that is protected via different mechanisms will
451 be critical to the development of next generation root-microbe-mineral ecosystem models
452 (Buchkowski, Bradford, Grandy, Schmitz, & Wieder, 2017). Protected C within CORPSE is
453 broadly defined and includes C that is physically inaccessible to microbes, C that is stabilized on
454 mineral surfaces. These contrast with C incorporated into chemically complex polymers that can
455 have moderately long turnover times (particularly in the absence of simple C inputs) but are not
456 physically protected from microbial access. In future studies, we recommend testing root-
457 microbe influences on decomposition of C that is protected by different mechanisms to advance
458 model development. While we demonstrated microbial use of recent C inputs, microbial use of C
459 inputs that have been incorporated into different pools of C is another important next step to
460 pursue. We suggest future investigations of microbial decomposition of isotopically labeled
461 particulate and mineral-associated organic C or C that is protected from microbial decomposition
462 via different mechanisms. For example, in an experiment by Haddix, Paul, and Cotrufo (2016)
463 leaf litter with isotopically distinct structural and metabolic components was decomposed and C
464 from metabolic components was traced into the mineral-associated C pool, while C from
465 structural components was traced into the particulate C pool. Other investigations like this are
466 needed to improve how microbial traits and processes are represented in C models.

467 Conclusions

468 Our model and experiment suggested that root-microbe interactions have different effects on
469 decomposition of complex compared to simple soil C. Roots stimulated decomposition of leaf
470 material and did not stimulate decomposition of starch in a broadleaf boreal ecosystem. It is
471 likely that complex C decomposition increased with root density because of microbial growth,
472 i.e., limitations of active microbial biomass limitation were alleviated. Simple C decomposition
473 probably did not respond to root density or root exudation because microbes could grow
474 efficiently on the simple substrate without requiring additional resources. These results provide
475 an important constraint for representation of rhizosphere interactions in soil C models,
476 suggesting that model structures should accommodate interactions among substrates, microbes,
477 and roots to accurately represent soil decomposition mechanisms. We urge future investigators to
478 isolate decomposition in SOC fractions using measurements that take advantage of microbial –
479 omics technologies and advanced soil chemical analyses to increase our understanding of how
480 root-microbe interactions influence turnover of different soil C pools. Clearly, roots influence
481 microbial C processing, but the specific mechanisms of root-microbe interactions have yet to be
482 fully explored and understood in the context of existing biogeochemical frameworks.

483

484 **Acknowledgements**

485 This work was funded by the U.S. Department of Energy, Office of Science, Office of Biological
486 and Environmental Research, Terrestrial Ecosystem Sciences Program under Award Number
487 DE-SC0010562. A Graduate Research grant to JAMM from the Ecology & Evolutionary
488 Biology Department at University of Tennessee contributed to this work. BS is supported under
489 award NA14OAR4320106 from the National Oceanic and Atmospheric Administration, U.S.
490 Department of Commerce. The statements, findings, conclusions, and recommendations are
491 those of the author(s) and do not necessarily reflect the views of the National Oceanic and
492 Atmospheric Administration, or the U.S. Department of Commerce. ORNL is managed by the
493 University of Tennessee-Battelle, LLC, under contract DE-AC05-00OR22725 with the US
494 Department of Energy. S. Patel, K. Rewcastle, and J. Henning assisted with sample collection
495 and processing. G. Wang and R. J. Norby of ORNL provided comments on experimental design
496 and the Soil Ecology group at University of New Hampshire commented on an initial manuscript
497 draft. The authors declare no competing interests.

498

499 **Author Contributions**

- 500 • JAMM, ATC, and MAM conceived and designed the study;
- 501 • JAMM and CMP conducted the field study and carried out laboratory analyses;
- 502 • JAMM conducted statistical analyses and led manuscript writing;
- 503 • BNS ran model simulations and contributed to manuscript writing.
- 504 All authors actively revised manuscript drafts and gave final approval for publication.
- 505

506 **Data Accessibility**

507 Data collected for this study are archived online with the Environmental Data Initiative

508 (<https://doi.org/10.6073/pasta/e611de3fe6cd24c8666df91f45cb89b7>). Model code is available on

509 Zenodo (<https://doi.org/10.5281/zenodo.3564527>).

510

Author Manuscript

511 **References**

- 512 Bell, C. W., Fricks, B. E., Rocca, J. D., Steinweg, J. M., McMahon, S. K., & Wallenstein, M. D.
513 (2013). High-throughput fluorometric measurement of potential soil extracellular enzyme
514 activities. *Journal of visualized experiments: JoVE*, 81, 50961. doi: 10.3791/50961
- 515 Bradshaw, C. J. A. & Warkentin, I.G. (2015). Global estimates of boreal forest carbon stocks and
516 flux. *Global and Planetary Change*, 128, 24-30. doi: 10.1016/j.gloplacha.2015.02.004
- 517 Brzostek, E. R., Dragoni, D., Brown, Z. A., & Phillips, R. P. (2015). Mycorrhizal type
518 determines the magnitude and direction of root-induced changes in decomposition in a
519 temperate forest. *New Phytologist*, 206(4), 1274-1282. doi: 10.1111/nph.13303
- 520 Buchkowski, R. W., Bradford, M. A., Grandy, A. S., Schmitz, O. J., & Wieder, W. R. (2017).
521 Applying population and community ecology theory to advance understanding of
522 belowground biogeochemistry. *Ecology Letters*, 20(2), 231-245. doi:10.1111/ele.12712
- 523 Clemmensen, K. E., Bahr, A., Ovaskainen, O., Dahlberg, A., Ekblad, A., Wallander, H., Stenlid,
524 J., ... Lindahl, B. D. (2013). Roots and associated fungi drive long-term carbon
525 sequestration in boreal forest. *Science*, 339(6127), 1615-1618. doi:
526 10.1126/science.1231923
- 527 Crow, S. E., Lajtha, K., Bowden, R. D., Yano, Y., Brant, J. B., Caldwell, B. A., & Sulzman, E.
528 W. (2009). Increased coniferous needle inputs accelerate decomposition of soil carbon in
529 an old-growth forest. *Forest Ecology and Management*, 258(10), 2224-2232. doi:
530 10.1016/j.foreco.2009.01.014
- 531 Crowther T. W., Todd-Brown, K. E. O., Rowe, C. W., Wieder, W. R., Carey, J. C., Machmuller,
532 M. B., Snoek, L. B., ... Bradford, M. A. (2016). Quantifying global soil carbon losses in
533 response to warming. *Nature*, 540(7631), 104-108. doi: 10.1038/nature20150
- 534 DeAngelis, K. M., Brodie, E. L., DeSantis, T. Z., Andersen, G. L., Lindow, S. E., & Firestone,
535 M. K. (2009). Selective progressive response of soil microbial community to wild oat
536 roots. *ISME Journal*, 3(2), 168-178. doi: 10.1038/ismej.2008.103
- 537 Drake, J. E., Darby, B. A., Giasson, M. A., Kramer, M. A., Phillips, R. P., & Finzi, A. C. (2013).
538 Stoichiometry constrains microbial response to root exudation-insights from a model and
539 a field experiment in a temperate forest. *Biogeosciences*, 10(2), 821-838. doi:
540 10.5194/bg-10-821-2013

541 Finzi, A. C., Abramoff, R. Z., Spiller, K. S., Brzostek, E. R., Darby, B. A., Kramer, M. A., &
542 Phillips, R. P. (2015) Rhizosphere processes are quantitatively important components of
543 terrestrial carbon and nutrient cycles. *Global Change Biology*. 21(5), 2082-2094. doi:
544 10.1111/gcb.12816.

545 Franzluebbers, A. J. (1999) Potential C and N mineralization and microbial biomass from intact
546 and increasingly disturbed soils of varying texture. *Soil Biology and Biochemistry*, 31(8),
547 1083-1090. doi: 10.1016/S0038-0717(99)00022-X

548 Haddix, M. L., Paul, E. A., & Cotrufo, M. F. (2016). Dual, differential isotope labeling shows
549 the preferential movement of simple plant constituents into mineral-bonded soil organic
550 matter. *Global Change Biology*, 22(6), 2301-2312. doi: 10.1111/gcb.13237

551 Hanson, P., Riggs, J., Dorrance, C., & Hook, L. (2011). SPRUCE environmental monitoring
552 data: 2010–2014. Carbon Dioxide Information Analysis Center, Oak Ridge National
553 Laboratory, US Department of Energy, Oak Ridge, TN. URL <http://mnspruce.ornl.gov/>.
554 [accessed 29 September 2016].

555 Hartley, I. P., Garnett, M. H., Sommerkorn, M., Hopkins, D. W., Fletcher, B. J.,
556 Sloan, V. L., Phoenix, G. K., & Wookey, P. A. (2012). A potential loss of carbon
557 associated with greater plant growth in the European Arctic. *Nature Climate Change*,
558 2(12), 875-879. doi: 10.1038/nclimate1575.

559 Hicks Pries, C. E. et al. (2018). Root litter decomposition slows with soil depth. *Soil Biology and*
560 *Biochemistry*, 125, 103-114. doi: 10.1016/j.soilbio.2018.07.002.

561 Holz, M., Aurangojeb, M., Kasimir, Å., Boeckx, P., Kuzyakov, Y., Klemetsson, L., & Rütting,
562 T. (2016). Gross nitrogen dynamics in the mycorrhizosphere of an organic forest soil.
563 *Ecosystems*, 19(2), 284-295. doi: 10.1007/s10021-015-9931-4

564 Jenkinson, D. & Rayner, J. (1977). The turnover of soil organic matter in some of the
565 Rothamsted classical experiments. *Soil Science*, 123(5), 298-305. doi:
566 10.1097/00010694-197705000-00005

567 Jobbágy, E. G. & Jackson, R. B. (2000). The vertical distribution of soil organic carbon and its
568 relation to climate and vegetation. *Ecological Applications*, 10(2), 423-436. doi:
569 10.1890/1051-0761(2000)010[0423:TVDOSO]2.0.CO;2

570 Johnson, D., Leake, J. R., & Read, D. J. (2001). Novel in-growth core system enables functional
571 studies of grassland mycorrhizal mycelial networks. *New Phytologist*, 152(3), 555-562.
572 doi: 10.1046/j.0028-646X.2001.00273.x

573 Keiluweit, M., Bougoure, J. J., Nico, P. S., Pett-Ridge, J., Weber, P. K., & Kleber, M. (2015).
574 Mineral protection of soil carbon counteracted by root exudates. *Nature Climate Change*,
575 5(6), 588-595. doi: 10.1038/nclimate2580

576 Kolka, R. K., Grigal, D. F., Nater, E. A., & Verry, E. S. (2001). Hydrologic cycling of mercury
577 and organic carbon in a forested upland-bog watershed. *Soil Science Society of America*
578 *Journal*, 65(3), 897-905. doi: 10.2136/sssaj2001.653897x

579 Kuzyakov, Y. (2010). Priming effects: Interactions between living and dead organic matter. *Soil*
580 *Biology & Biochemistry*, 42(9), 1363-1371. doi: 10.1016/j.soilbio.2010.04.003

581 Langley, J. A., Chapman, S. K., & Hungate, B. A. (2006). Ectomycorrhizal colonization slows
582 root decomposition: the post-mortem fungal legacy. *Ecology Letters*, 9(8), 955-959. doi:
583 10.1111/j.1461-0248.2006.00948.x

584 Lawrence, C. R., Neff, J. C., & Schimel, J. P. (2009). Does adding microbial mechanisms of
585 decomposition improve soil organic matter models? A comparison of four models using
586 data from a pulsed rewetting experiment. *Soil Biology & Biochemistry*, 41(9), 1923-
587 1934. doi: 10.1016/j.soilbio.2009.06.016

588 Li, X., Zhu, J., Lange, H., and Han, S. (2012). A modified ingrowth core method for measuring
589 fine root production, mortality and decomposition in forests. *Tree Physiology*, 33(1), 18-
590 25. doi: 10.1093/treephys/tps124

591 Lindahl, B. D., de Boer, W., & Finlay, R. D. (2010). Disruption of root carbon transport into
592 forest humus stimulates fungal opportunists at the expense of mycorrhizal fungi. *ISME*
593 *Journal*, 4(7), 872-881. doi: 10.1038/ismej.2010.19

594 Lobet, G. & Draye, X. (2013). Novel scanning procedure enabling the vectorization of entire
595 rhizotron-grown root systems. *Plant Methods*, 9(1), 1. doi: 10.1186/1746-4811-9-1

596 Lou, Y., Clay, S. A., Davis, A. S., Dille, A., Felix, J., Ramirez, A. H. M., Sprague, C. L., &
597 Yannarell, A. C. (2014). An affinity-effect relationship for microbial communities in
598 plant-soil feedback loops. *Microbial Ecology*, 67(4), 866-876. doi: 10.1007/s00248-013-
599 0349-2

600 Lynch, D. J., Matamala, R., Iversen, C. M., Norby, R. J., & Gonzalez-Meler, M. A. (2013).
601 Stored carbon partly fuels fine-root respiration but is not used for production of new fine
602 roots. *New Phytologist*, 199(2), 420-430. doi: 10.1111/nph.12290

603 McCormack, M. L., Dickie, A. D., Eissenstat, M., Fahey, T. J., Fernandez, C. W., Guo, D.,
604 Helmisaari, H. S., ... Jackson, R. B. (2015). Redefining fine roots improves
605 understanding of below-ground contributions to terrestrial biosphere processes. *New*
606 *Phytologist*, 207(3), 505-518. doi: 10.1111/nph.13363

607 Meier, I. C., Finzi, A. C., & Phillips, R. P. (2017). Root exudates increase N availability by
608 stimulating microbial turnover of fast-cycling N pools. *Soil Biology & Biochemistry*,
609 106, 119-128. doi: 10.1016/j.soilbio.2016.12.004

610 Moore, J. A. M., Jiang, J., Patterson, C. M., Mayes, M. A., Wang, G., & Classen, A. T. (2015).
611 Interactions among roots, mycorrhizas and free-living microbial communities
612 differentially impact soil carbon processes. *Journal of Ecology*, 103(6), 1442-1453. doi:
613 10.1111/1365-2745.12484

614 Parton, W. J., Hartman, M., Ojima, D., & Schimel, D. (1998). DAYCENT and its land surface
615 submodel: description and testing. *Global and Planetary Change*, 19(1-4), 35-48. doi:
616 10.1016/s0921-8181(98)00040-x

617 Parton, W. J., Stewart, J. W. B., & Cole, C. V. (1988). Dynamics of C, N, P, and S in grassland
618 soils - a model. *Biogeochemistry*, 5(1), 109-131. doi: 10.1007/bf02180320

619 Phillips, R. P., Finzi, A. C., & Bernhardt, E. S. (2011). Enhanced root exudation induces
620 microbial feedbacks to N cycling in a pine forest under long-term CO₂ fumigation.
621 *Ecology Letters*, 14(2), 187-194. doi: 10.1111/j.1461-0248.2010.01570.x

622 Phillips, R. P., Meier, I. C., Bernhardt, E. S., Grandy, A. S., Wickings, K., & Finzi, A. C. (2012).
623 Roots and fungi accelerate carbon and nitrogen cycling in forests exposed to elevated
624 CO₂. *Ecology Letters*, 15(9), 1042-1049. doi: 10.1111/j.1461-0248.2012.01827.x

625 Post, W. M., Emanuel, W. R., Zinke, P. J., & Stangenberger, A. G. (1982). Soil carbon pools and
626 world life zones. *Nature*, 298(5870), 156-159. doi: 10.1038/298156a0

627 R Core Team (2014). fBasics: Rmetrics - Markets and Basic Statistics. R package version
628 3011.87.

629 R Core Team (2014). R: A language and environment for statistical computing. R Foundation for
630 Statistical Computing, Vienna, Austria, 2012. ISBN 3-900051-07-0.

631 Rasse, D. P., Rumpel, C., & Dignac, M.-F. (2005). Is soil carbon mostly root carbon?
632 Mechanisms for a specific stabilisation. *Plant and Soil*, 269(1), 341-356. doi:
633 10.1007/s11104-004-0907-y

634 Rewcastle, K. E., Moore, J. A. M., Henning, J. A., Mayes, M. A., Patterson, C. M., Wang, G.,
635 Metcalfe, D. B., & Classen, A. T. 2019. Investigating drivers of microbial activity and
636 respiration in a forested bog. *Pedosphere* In press

637 Schimel, J. (2013). Soil carbon: microbes and global carbon. *Nature Climate Change* 3(10):867-
638 868. doi: 10.1038/nclimate2015

639 Schimel, J. P., & Weintraub, M. N. (2003). The implications of exoenzyme activity on microbial
640 carbon and nitrogen limitation in soil: a theoretical model. *Soil Biology & Biochemistry*,
641 35(4), 549-563. doi: 10.1016/s0038-0717(03)00015-4

642 Shi, S., Richardson, A. E., O'Callaghan, M., DeAngelis, K. M., Jones, E. E., Stewart, A.,
643 Firestone, M. K., & Condon, L. M. (2011). Effects of selected root exudate components
644 on soil bacterial communities. *FEMS Microbiology Ecology*, 77(3), 600-610. doi:
645 10.1111/j.1574-6941.2011.01150.x

646 Six, J., Bossuyt, H., Degryze, S., and Denef, K. (2004). A history of research on the link between
647 (micro)aggregates, soil biota, and soil organic matter dynamics. *Soil and Tillage*
648 *Research*, 79, 7-31. doi: 10.1016/j.still.2004.03.008

649 Sulman, B. N., Phillips, R. P., Oishi, A. C., Shevliakova, E., & Pacala, S. W. (2014). Microbe-
650 driven turnover offsets mineral-mediated storage of soil carbon under elevated CO₂.
651 *Nature Climate Change*, 4(12), 1099-1102. doi: 10.1038/nclimate2436

652 Sulman, B. N., Shevliakova, E., Brzostek, E. R., Kivlin, S. K., Malyshev, S., Menge, D. N. L.,
653 and Zhang, X. (2019). Diverse mycorrhizal associations enhance terrestrial C storage in a
654 global model. *Global Biogeochemical Cycles*, 33(4), 501-523. doi:
655 10.1029/2018GB005973

656 Tang, J. Y. (2015). On the relationships between the Michaelis–Menten kinetics, reverse
657 Michaelis–Menten kinetics, equilibrium chemistry approximation kinetics, and quadratic
658 kinetics. *Geoscientific Model Development*, 8, 3823-3835. doi: 10.5194/gmd-8-3823-
659 2015

660 Taylor, K. E., Stouffer, R. J., & Meehl, G. A. (2012). An Overview of CMIP5 and the
661 Experiment Design. *Bulletin of the American Meteorological Society*, 93(4), 485-498.
662 doi: 10.1175/bams-d-11-00094.1

663 Todd-Brown, K. E. O., Hopkins, F. M., Kivlin, S. N., Talbot, J. M., & Allison, S. D. (2012). A
664 framework for representing microbial decomposition in coupled climate models.
665 *Biogeochemistry*, 109(1-3), 19-33. doi: 10.1007/s10533-011-9635-6

666 Todd-Brown, K. E. O., Randerson, J. T., Post, W. M., Hoffman, F. M., Tarnocai, C., Schuur, E.
667 A. G., & Allison, S. D. (2013). Causes of variation in soil carbon simulations from
668 CMIP5 Earth system models and comparison with observations. *Biogeosciences*, 10(3),
669 1717-1736. doi: 10.5194/bg-10-1717-2013

670 Treseder, K. K., & Lennon, J. T. (2015). Fungal traits that drive ecosystem dynamics on land.
671 *Microbiology and Molecular Biology Reviews*, 79(2), 243-262. doi:
672 10.1128/MMBR.00001-15

673 Treseder, K. K., Balsler, T. C., Bradford, M. A., Brodie, E. L., Dubinsky, E. A., Eviner, V. T.,
674 Hofmockel, K. S., ... Waldrop, M. P. (2012). Integrating microbial ecology into
675 ecosystem models: challenges and priorities. *Biogeochemistry*, 109(1-3), 7-18. doi:
676 10.1007/s10533-011-9636-5

677 Vance, E., Brookes, P., & Jenkinson, D. (1987). An extraction method for measuring soil
678 microbial biomass C. *Soil Biology & Biochemistry*, 19(6), 703-707. doi: 10.1016/0038-
679 0717(87)90052-6

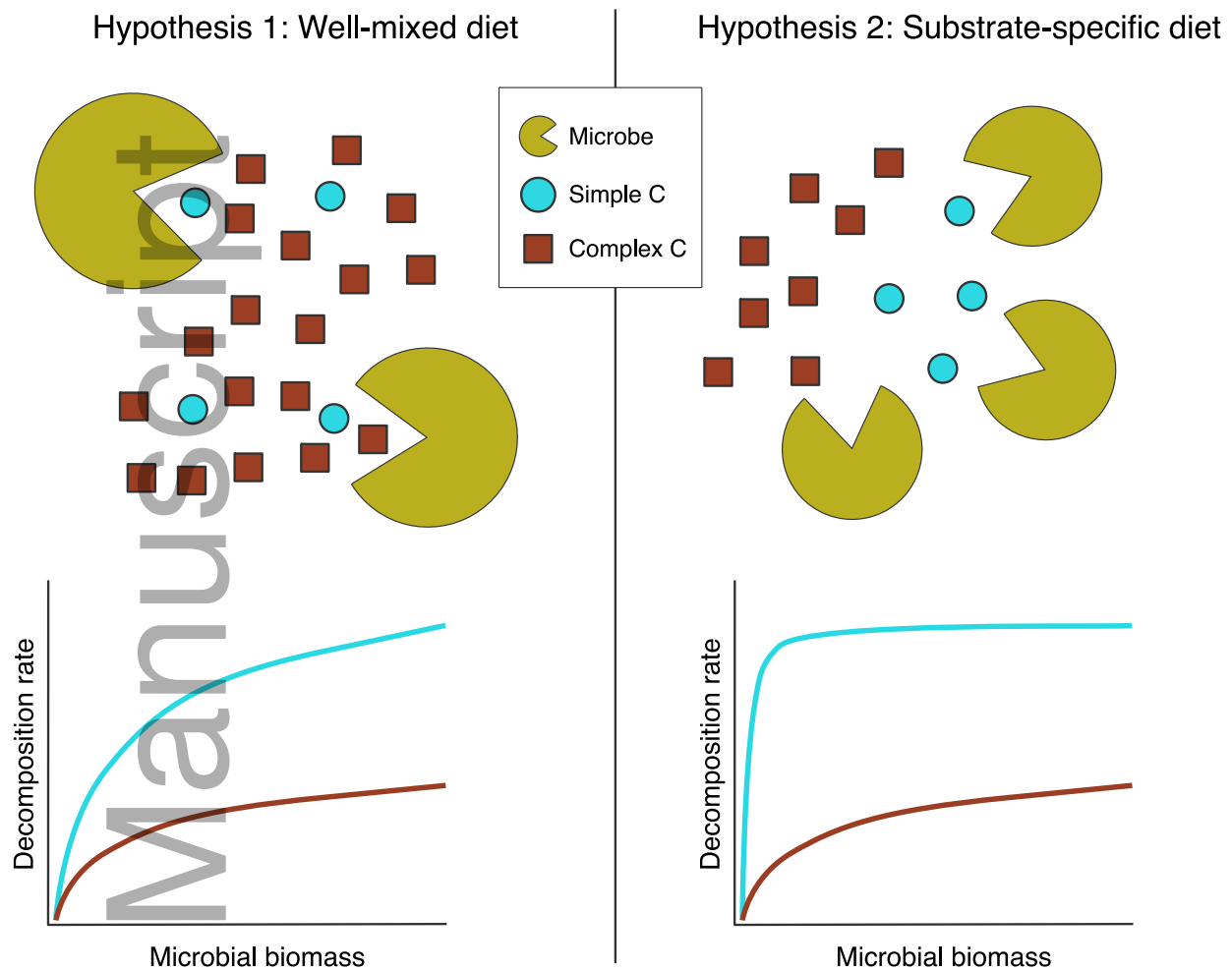
680 Vogt, K. A., Vogt, D. J., Palmiotto, P. A., Boon, P., O'Hara, J., & Asbjornsen, H. (1995). Review
681 of root dynamics in forest ecosystems grouped by climate, climatic forest type and
682 species. *Plant and Soil*, 187(2), 159-219. doi: 10.1007/bf00017088

683 Voroney, R., Brooks, P. C., & Beyaert, R. (2007). Soil microbial biomass C, N, P, and S. In: M.
684 R. Carter & E. G. Gregorich, (Eds.), *Soil Sampling and Methods of Analysis*, Second
685 Edition (pp. 637-652). Boca Raton, FL: CRC Press.

686 Wang, G., Jagadamma, S., Mayes, M. A., Schadt, C. W., Steinweg, J. M., Gu, L., & Post, W. M.
687 (2015). Microbial dormancy improves development and experimental validation of
688 ecosystem model. *ISME Journal*, 9(1), 226-237. doi: 10.1038/ismej.2014.120

- 689 Xu, S., Liu, L. L., & Sayer, E. J. (2013). Variability of above-ground litter inputs alters soil
690 physicochemical and biological processes: a meta-analysis of litterfall-manipulation
691 experiments. *Biogeosciences*, 10(11), 7423-7433. doi: 10.5194/bg-10-7423-2013
- 692 Xu, X., Schimel, J. P., Thornton, P. E., Song, X., Yuan, F., & Goswami, S. (2014). Substrate and
693 environmental controls on microbial assimilation of soil organic carbon: a framework for
694 Earth system models. *Ecology Letters*, 17(5), 547-555. doi: 10.1111/ele.12254
- 695 Yin, H., Li, Y., Xiao, J., Xu, Z., Cheng, X., & Liu, Q. (2013). Enhanced root exudation
696 stimulates soil nitrogen transformations in a subalpine coniferous forest under
697 experimental warming. *Global Change Biology*, 19(7), 2158-2167. doi:
698 10.1111/gcb.12161
- 699 Zak, D. R., & Kling, G. W. (2006). Microbial community composition and function across an
700 arctic tundra landscape. *Ecology*, 87(7), 1659-1670. doi: 10.1890/0012-
701 9658(2006)87[1659:mccafa]2.0.co;2

Author Manuscript



703

704 Figure 1: We simulated two hypothetical frameworks using the CORPSE model of C pools and

705 flows. In Hypothesis 1, we structured CORPSE to allow microbial breakdown of a mixture of

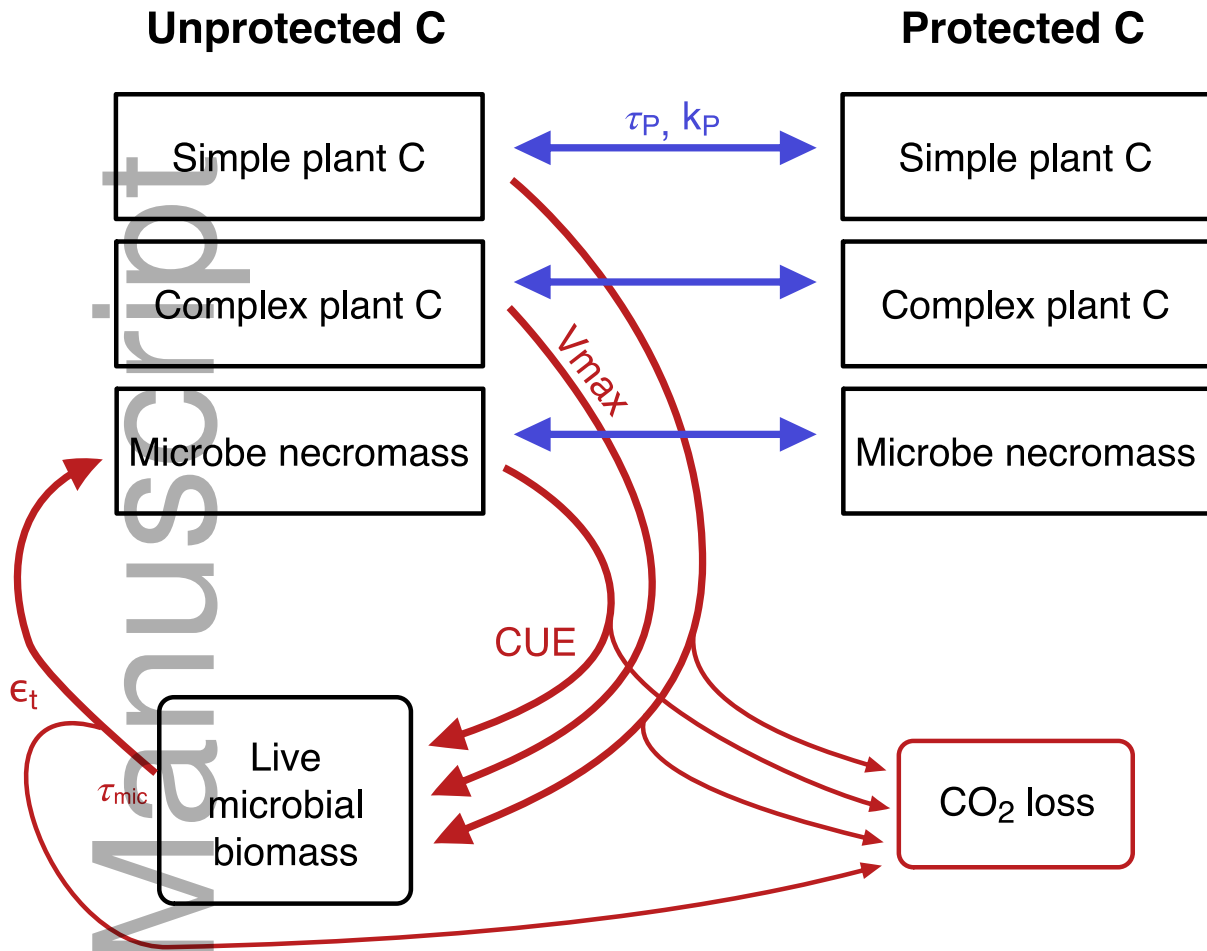
706 substrates with low substrate affinity. In Hypothesis 2, we structured CORPSE to restrict

707 microbial access to particular substrate types with high substrate fidelity. The relationship

708 between microbial biomass and substrate fidelity was expected to have consequences for the

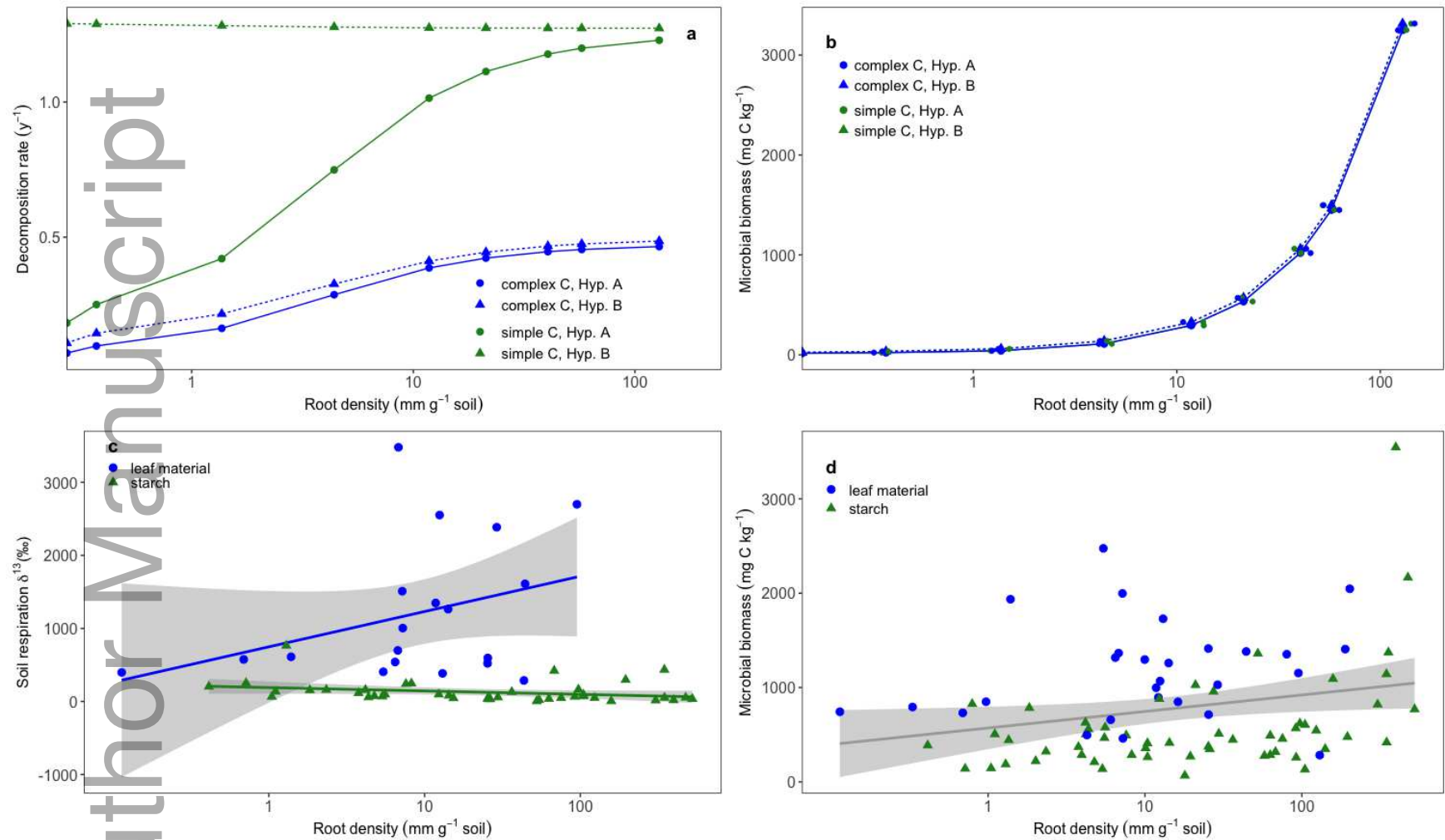
709 degree of saturation of decomposition rates with increasing microbial biomass.

710



711
 712 Figure 2: Carbon pools (boxes) and flows (arrows) in the CORPSE model. Plants assimilate
 713 carbon and transfer simple and complex C to microbes. Plant C and microbial necromass C can
 714 be unprotected and available for microbial uptake, or in a protected pool that is unavailable for
 715 microbial uptake. Flow of C between protected and unprotected pools occurs at a slow but
 716 constant rate. C flow into live microbial biomass contributes to growth of that pool, is released as
 717 CO₂, or contributes to the microbial necromass pool. Parameters that were modified to test the
 718 model structural hypotheses included microbial enzyme kinetics (k_P and V_{max}) and microbial C
 719 use efficiency (CUE). Our rhizosphere manipulation experiment used isotope tracers to track C
 720 flow from simple and complex pools through to CO₂ loss, or soil respiration. See the CORPSE
 721 Simulations section for a detailed model description and equations and Supplemental Table 2 for
 722 model parameters.

723

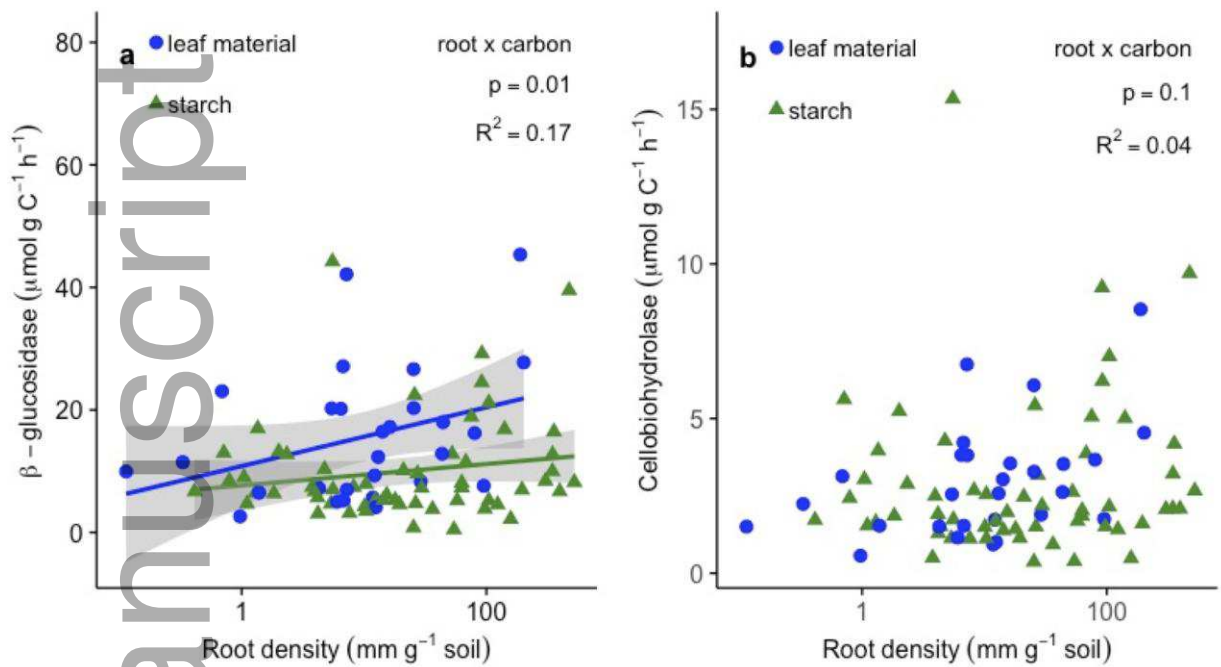


724

725 Figure 3: Relationships between root density, decomposition rate, and microbial biomass in model simulations (a, b), and between root
 726 density, soil respiration, and microbial biomass in the field experiment (c, d). The decomposition rate per unit mass for complex C
 727 (blue) and simple C (green) in CORSPE is shown relative to simulations with zero root exudation (i.e., plant simple C inputs) and as a

728 function of root density (a). Results from CORPSE simulations are shown for Hypothesis A (circles) and Hypothesis B (triangles).
729 Simulated microbial biomass as a function of root density (b). ^{13}C -labeled leaf material (blue circles) and ^{13}C -labeled starch (green
730 triangles) as a function of increasing root density (c). Microbial biomass as a function of increasing root length, for ^{13}C -labeled leaf
731 material (blue circles) and ^{13}C -labeled starch (green triangles) (d).

Author Manuscript



732

733 Figure 4: The carbon-degrading enzymes β -glucosidase (a) and cellobiohydrolase (b) as a
 734 function of increasing root density. Enzyme activity was measured in soils amended with leaf
 735 material (blue circles) and starch (green triangles).